Association between intracranial vascular vulnerability and indirect revascularization development in moyamoya disease

Haruto Uchino, Masaki Ito, Kota Kurisu, Taku Sugiyama, Miki Fujimura

Department of Neurosurgery, Hokkaido University Graduate School of Medicine, Sapporo, Japan

Corresponding Author:

Haruto Uchino, MD, PhD

Department of Neurosurgery,

Hokkaido University Graduate School of Medicine,

North 15 West 7, Kita-ku, Sapporo 060-8638, Japan

Tel: +81-11-706-5987

Fax: +81-11-708-7737

E-mail: uchinohr@gmail.com

ORCID ID: 0000-0001-6567-8136

Abstract

Negative remodeling, characterized by a decrease in the outer diameter of cerebral arteries, is a hallmark of moyamoya disease (MMD). Postoperative fluid-attenuated inversion recovery (FLAIR) cortical hyperintensity (FCH), indicative of leptomeningeal vasogenic edema, and indirect bypass development are also distinctive features. We investigated the relationships between negative remodeling and these postoperative phenomena. We analyzed 42 hemispheres from 37 adult patients with MMD who underwent combined direct and indirect revascularization. Negative remodeling was assessed by measuring the terminal portion (C1) vessel diameter of the internal carotid artery on preoperative heavy T2-weighted images. FCH was scored from 0 to 6 based on its extent on FLAIR images obtained 2 days postoperatively; indirect bypass development was evaluated qualitatively using magnetic resonance angiography 6 months post-surgery. The participants' median age was 45 years; 76% were female and 90% presented with ischemic onset. The median C1 diameter was 2.39 mm, median FCH score was 2.5, and favorable indirect bypass development was observed in 64% of cases. Smaller preoperative C1 diameters (2.27 mm vs. 3.02 mm, $p<0.0001$) and higher FCH scores (median 3 vs. 2, $p<0.05$) correlated with favorable indirect bypass development. Smaller C1 diameters also aligned with extensive FCH (2.94 mm vs. 2.20 mm, $p<0.001$). Multivariate analysis revealed a significant association between reduced preoperative C1 diameter and favorable indirect bypass development (odds ratio 0.019, 95% confidence interval 0.010–0.17, $p<0.01$). These findings suggest that advanced intracranial vascular remodeling in MMD correlates with vascular vulnerability and favorable indirect bypass development.

Keywords: moyamoya disease, negative remodeling, indirect bypass, FLAIR cortical hyperintensity, vascular vulnerability

Introduction

Moyamoya disease (MMD) is a steno-occlusive cerebrovascular disorder characterized by progressive supraclinoid internal carotid artery (ICA) occlusion and abnormal vascular network formation [1-3]. Recent vessel wall imaging studies have revealed that a decrease in the outer diameter of the carotid fork, alongside inner lumen stenosis, is a characteristic phenomenon of MMD [4, 5]. This vascular negative remodeling progresses with advancing disease stage [4, 6, 7]. Thus, this finding has been incorporated into the latest diagnostic criteria for MMD, published by the Research Committee on Moyamoya Disease of the Ministry of Health, Welfare, and Labor of Japan [8].

Abnormal hyperintensity on fluid-attenuated inversion recovery (FLAIR), termed FLAIR cortical hyperintensity (FCH), is a characteristic finding frequently observed in the acute period after direct revascularization surgery for MMD. Extensive FCH has been associated with transient neurological deficits and cerebral hyperperfusion syndrome [9-11]. Vasogenic edema of the brain surface, driven by hemodynamic changes, is considered an underlying mechanism of FCH [9, 12]. Indirect bypass development in the chronic postoperative period is another characteristic feature of MMD. Favorable indirect bypass development is observed in over 90% of children and approximately 60–80% of adults undergoing combined direct and indirect bypass surgery [13, 14].

Vascular negative remodeling is a characteristic phenomenon of MMD. FCH and indirect bypass development are also characteristic postoperative features. We hypothesized that these phenomena share a common pathological background. Our previous studies demonstrated associations between *RNF213*—a risk gene for MMD that contributes to vascular vulnerability—and these phenomena [9, 15-18]. However, their precise mechanisms and interrelations remain unclear. Therefore, in this study, we aimed to evaluate the associations between these phenomena in MMD.

Materials and Methods

Patients

We retrospectively analyzed consecutive adult patients (aged >18 years) diagnosed with MMD, excluding those with moyamoya syndrome. These patients underwent *RNF213* p.R4810K genetic analysis and combined direct–indirect bypass surgery at Hokkaido University Hospital between January 2021 and September 2024. The diagnosis followed the guidelines established by the Research Committee on Moyamoya Disease under the Ministry of Health, Labor, and Welfare of Japan [8]. Catheter-based cerebral angiography was used for definitive MMD diagnosis, and the Suzuki disease stage was determined, ranging from 0 (normal) to 6 (advanced) [1].

This study was approved by an Institutional Review Board at Hokkaido University Hospital (approval number 024-0257). Informed consent was obtained from all individual participants included in the study.

Surgical procedures

Surgical revascularization was considered for patients with hemodynamic compromise or hemorrhagic presentation based on Japanese guidelines [3]. The surgical procedure has been previously described [19]. In our approach, we universally perform a combined direct and indirect bypass, regardless of the patient's age. The direct bypass consists of a single superficial temporal artery (STA)–middle cerebral artery (MCA) anastomosis. After performing an approximately 8 cm craniotomy near the Sylvian fissure, the dura is carefully opened while preserving the main branch of the middle meningeal artery. The parietal branch of the STA is then anastomosed to the cortical branch of the MCA. The dura is inverted and placed on the brain surface, and the temporal muscle is sutured to the dural edge, thereby facilitating indirect revascularization through the encephalo-duro-myo-synangiosis procedure.

Genetic analysis of the RNF213 p.R4810K polymorphism

Peripheral blood samples were obtained from the patients, and the TaqMan single-nucleotide polymorphism genotyping assay (Applied Biosystems, Foster City, CA, USA) was used to determine the germline *RNF213* p.R4810K allelic type, as described previously [16, 17]. Participants were then classified into *RNF213* mutant (homozygous or heterozygous) and wild-type groups.

Preoperative measurement of C1 outer diameter

Preoperative evaluation of the outer diameter of intracranial arteries was performed using 3.0-tesla magnetic resonance (MR) scanners and constructive interference in steady-state (CISS) imaging with the following parameters: repetition time, 4.9–7.2 ms; echo time, 2.3–3.6 ms; field of view, 180–230 mm; acquisition matrix, 288–384 × 260–384 (reconstructed matrix, 512–760 × 512–760); slice thickness, 0.6–1.2 mm (slice spacing, 0.3–1.0 mm); and 220–400 slices. Images were acquired in the sagittal plane, and three-dimensional planes were subsequently reconstructed. The outer diameter was precisely measured at the terminal ICA (C1) portion just proximal to the bifurcation, using an image viewer (**Fig. 1**).

Evaluation of FCH

Preoperative and postoperative day 2 MR studies, including FLAIR imaging, were routinely performed. FCH was defined as intraparenchymal hyperintensity in the cortex of the surgically treated hemisphere on FLAIR images (**Fig. 1**). The extent of FCH was assessed across all slices of axial FLAIR images. The FCH score was determined as previously described [9, 10]. The frontal lobe was classified as the anterior region, while the parietal and temporal lobes were classified as the posterior region. For each region, the extent of FCH was scored as follows: 0 (not visible), 1 (limited to one-third), 2 (extending from one-third to two-thirds), or 3 (extending beyond two-thirds). The total FCH score was the sum of the anterior and posterior scores, ranging from a minimum of 0 to a maximum of 6. The FCH scores were determined by consensus between two authors (HU and MI).

Evaluation of bypass development with MRA

We used MR angiography (MRA) to evaluate bypass development, as previously reported [13, 16, 17]. MRA was performed preoperatively and during follow-up, which occurred over 6 months later. For direct bypasses, we evaluated the patency of the donor STA. For indirect bypasses, we evaluated the middle meningeal artery or deep temporal artery during follow-up. Indirect bypass development was considered favorable if these arteries were enlarged compared with their preoperative size. If the arteries showed no change or became smaller, indirect bypass development was considered poor (**Fig. 1**). MRA findings were reviewed by two authors (HU and MI), and a consensus was reached.

Perioperative cerebral blood flow measurements

We used 123I N-isopropyl-p-iodoamphetamine single-photon emission CT (SPECT) to assess cerebral blood flow (CBF) preoperatively and on postoperative days 1 and 7. Radiological hyperperfusion was defined as a focal and intense increase in CBF on SPECT. Among them, symptomatic hyperperfusion was diagnosed when radiological hyperperfusion on SPECT corresponded to an area of neurological deficits without new ischemic lesions [20, 21].

Data analyses

Baseline characteristics, including age, sex, disease onset type, Suzuki disease stage, preoperative and postoperative modified Rankin Scale (mRS) scores, and *RNF213* genotype, were collected. The Mann–Whitney U test was used to compare continuous and ranked variables between groups, while g the $\chi 2$ test was used to compare categorical variables. A multivariate logistic regression analysis was conducted to assess the effects of clinical parameters on indirect bypass development, incorporating parameters that achieved $p<0.05$ in the univariate analysis. The significance level was set at $p<0.05$. Receiver operating characteristic (ROC) analysis was performed to evaluate the diagnostic value of the preoperative C1 outer diameter for predicting indirect bypass development. Statistical analyses were performed using GraphPad Prism (GraphPad Software, San Diego, CA, USA).

Results

Demographic data

A total of 42 hemispheres from 37 adult patients with MMD were analyzed. Clinical data at both the patient and hemisphere levels, including median age, sex, initial presentation, *RNF213* genotype, and Suzuki disease stage, are presented in **Table 1**. The median C1 diameter was 2.39 mm, while the median FCH score was 2.5. The patency of direct bypass was confirmed in all cases. Favorable indirect bypass development was observed in 64% of the hemispheres (**Table 1**). Preoperative mRS scores were 0 in 34 cases, 1 in six cases, and 2 in two cases. By postoperative day 14, the mRS scores remained unchanged in all cases except one, in which a postoperative hemorrhagic stroke led to a worsening of the mRS score from 0 to 2.

Associations of C1 outer diameter, FCH score, and indirect bypass development

The C1 outer diameter was significantly smaller in hemispheres with favorable indirect bypass development than in those with poor development (median [IQR]: 2.27 [2.04–2.39] vs. 3.02 [2.49–3.56], $p<0.0001$, **Fig. 2A**). The FCH score was significantly higher in hemispheres with favorable indirect bypass development than in those with poor development (median [IQR]: 3 [2–4] vs. 2 [0–3], $p<0.05$, **Fig. 2B**). Then, the relationship between C1 outer diameter and FCH was analyzed by categorizing FCH scores into three groups: 0–1, 2–3, and 4–5. The C1 outer diameter was significantly smaller in hemispheres with higher FCH scores than in those with lower FCH scores. Specifically, the C1 outer diameter was significantly smaller in hemispheres with FCH scores of 2–3 and 4–5 than in those with FCH scores of 0–1 (median [IQR]: 2.39 [2.11–2.79] vs. 2.94 [2.49–3.14], $p<0.05$; and 2.20 [1.98–2.31] vs. 2.94 [2.49–3.14], $p<0.001$, respectively; **Fig. 2C**). Furthermore, the C1 outer diameter was significantly smaller in hemispheres with high FCH scores (4–5) and favorable indirect bypass development than in those with low FCH scores (0–1) and poor indirect bypass development (2.20 [2.01–2.29] mm vs. 3.10 [2.73–3.14] mm, $p<0.001$). These findings demonstrate an association between these characteristic MMD phenomena.

We further examined several factors associated with favorable indirect revascularization following combined bypass in adults with MMD. In this study, postoperative hyperperfusion was observed in 11 cases, including nine cases of radiological hyperperfusion and two cases of symptomatic hyperperfusion. As mentioned above, univariate analysis revealed that C1 outer diameter and FCH score correlated with favorable indirect bypass development. Multiple logistic regression analysis identified C1 outer diameter as an independent predictor of favorable indirect bypass development (OR, 0.019; 95% CI, 0.0010–0.17; $p<0.01$, **Table 2**).

Prediction of indirect bypass development using C1 outer diameter

We evaluated the accuracy of predicting favorable indirect bypass development based on the preoperative C1 outer diameter. ROC analysis identified an optimal threshold of 2.53 mm for the C1 outer diameter, with a specificity of 0.73 and a sensitivity of 0.89. The area under the curve was 0.87 (**Fig. 3**).

Discussion

To the best of our knowledge, this is the first study to investigate the associations among C1 negative remodeling, FCH, and indirect bypass development in MMD. Our findings indicate that the preoperative degree of C1 negative remodeling and the extent of FCH were each correlated with favorable indirect bypass development in the chronic phase after surgery, as shown in the univariate analysis. Additionally, preoperative progression of C1 negative remodeling and wider FCH were associated with each other. Multivariate and ROC analyses demonstrated that a decreased preoperative C1 outer diameter was an independent predictor of favorable indirect bypass development. Thus, preoperative C1 outer diameter may serve as a potential marker to guide tailored surgical revascularization strategies for MMD in the future.

In 2002, Komiyama et al. reported a decrease in the outer diameter of the terminal ICA in MMD using CISS imaging [5]. Subsequently, Kaku et al. quantitatively analyzed the outer diameters of C1 and M1 using CISS imaging and demonstrated that these diameters were significantly smaller in MMD than in atherosclerotic disease [22]. In their study, the mean C1 outer diameters in the MMD, atherosclerosis, and control groups were 2.61 mm, 4.32 mm, and 4.04 mm, respectively. Moreover, previous studies have shown that vascular negative remodeling is a characteristic phenomenon of MMD [4, 6, 7, 22, 23]. Histopathological findings of the terminal ICA in MMD include thickening of the intima, tortuosity of the internal elastic lamina, and attenuation of the media [2, 24, 25]. Similar findings, including a thickened intima and a thinned media, have also been observed in distal MCA specimens obtained during bypass surgery [26, 27]. These characteristic histopathological features suggest that vascular negative remodeling and vascular vulnerability extend beyond the proximal portions to the distal cerebral arteries.

FCH is frequently observed in over 80% of cases during the acute phase following surgery for MMD [9, 10, 12]. The underlying mechanisms of FCH development after revascularization surgery for MMD are not fully understood. However, vasogenic edema is predominantly involved in this intrinsic phenomenon, characterized by blood–brain barrier (BBB) dysfunction and fluid leakage into the brain parenchyma [9, 12]. Several studies suggest that the intrinsic vascular vulnerability in MMD may contribute to the formation of vasogenic edema or FCH after revascularization surgery. First, compared with healthy individuals, patients with MMD showed significantly higher expression of vascular

endothelial growth factor (VEGF) and matrix metalloproteinase 9 in blood samples, both of which are known to increase permeability of the BBB [28, 29]. Second, intraoperative video angiography has demonstrated sodium fluorescein extravasation in MMD patients, indicating BBB impairment [30]. Third, we recently reported that *RNF213* p.R4810K, which may lead to functional impairment of endothelial cells [31, 32], was significantly associated with prolonged FCH. Fourth, the aforementioned histological analysis of MCA specimens obtained during surgery suggests anatomical fragility in the intracranial arteries of MMD patients [26, 27]. These findings align with the results of previous reports indicating that MMD patients, particularly adults with advanced Suzuki disease stages, are at a higher risk of developing cerebral hyperperfusion syndrome after direct revascularization surgery than non-MMD patients undergoing similar procedures [33, 34].

The development of an indirect bypass involves angiogenesis between the ischemic brain surface and donor tissues. Previous studies have analyzed the mechanisms of indirect bypass development in the ischemic brain using animal models [35, 36]. In the early stages of angiogenesis, high BBB permeability significantly contributes to the effective angiogenic sprouting of endothelial cells [37]. Notably, the administration of VEGF, an angiogenic factor known to enhance vascular permeability, in combination with encephalo-myo-synangiosis surgery, has been shown to promote angiogenesis between the brain and temporal muscle in animal models [38, 39]. Therefore, we propose that vascular negative remodeling is comparable to vascular vulnerability and is associated with both FCH and indirect bypass development, with vascular permeability playing a central role in this process.

This study has some limitations. First, it was a retrospective analysis conducted at a single institution with a limited number of cases. Variations in surgical procedures for MMD across institutions, such as the number of bypasses performed and the extent of craniotomy, may have influenced the results. Additionally, other potential confounding factors may have also affected our findings. Subgroup analysis was not feasible due to the small sample size. Further studies with larger cohorts across multiple institutions are needed to validate these findings. Second, this study did not include in vitro investigations into the common mechanisms underlying vascular negative remodeling, FCH, and indirect bypass

development. Thus, while previous studies support the relevance of our findings, this study does not directly demonstrate the biological mechanisms underlying these phenomena.

Third, negative remodeling was assessed using the C1 outer diameter. However, quantitatively evaluating the vulnerability of peripheral cerebral arteries with radiological imaging remains challenging, and remodeling in these arteries was not analyzed. Further studies are warranted to clarify the direct relationship between C1 negative remodeling and peripheral cerebral artery vulnerability, as suggested by the presence of FCH.

Conclusion

Preoperative advanced C1 remodeling in MMD was associated with vascular vulnerability and favorable indirect bypass development. The progression of intracranial vascular negative remodeling may be linked to a leptomeningeal environment that facilitates indirect bypass development, as suggested by the increased vascular permeability observed in postoperative FCH.

Figure Legends

Fig. 1 Representative images of preoperative MRA and CISS, as well as postoperative FLAIR and MRA. Case 1: Preoperative CISS showing shrinkage or negative remodeling of C1 (diameter: 2.31 mm, arrow). Postoperative FLAIR showing a wide area of FCH (FCH score: 5) in the operated hemisphere (dotted circle) and MRA at 6 months postoperatively demonstrating favorable indirect bypass development (deep temporal artery, arrowheads). Case 2: Preoperative CISS showing a C1 diameter of 3.14 mm, with less advanced negative remodeling (diameter: 3.14 mm, arrow). Postoperative FLAIR does not show FCH (FCH score: 0) in the operated hemisphere, and MRA at 6 months postoperatively demonstrates poor indirect bypass development despite favorable direct bypass patency.

Abbreviations: CISS, constructive interference in steady-state; FCH, FLAIR cortical hyperintensity; FLAIR, fluid-attenuated inversion recovery; MRA, magnetic resonance angiography

Fig. 2 Box plots illustrating the relationships between indirect bypass development and C1 outer diameter (A) and FCH score (B), as well as between C1 outer diameter and FCH score (C).

The dots and error bars indicate the median and interquartile range of outer diameters, respectively. *p<0.05, ***p<0.001, ****p<0.0001

Abbreviations: FCH, fluid-attenuated inversion recovery cortical hyperintensity

Fig. 3 Receiver operating characteristic (ROC) curve representing the diagnostic accuracy of C1 outer diameter for predicting favorable indirect bypass development. For a threshold value of 2.53 mm, the specificity and sensitivity are 0.73 and 0.89, respectively. The area under the curve is 0.87.

References

1. Suzuki J, Takaku A (1969) Cerebrovascular "moyamoya" disease. Disease showing abnormal net-like vessels in base of brain. Arch Neurol 20:288-299. https://doi.org/10.1001/archneur.1969.00480090076012
2. Fujimura M, Tominaga T (2015) Diagnosis of moyamoya disease: international standard and regional differences. Neurol Med Chir (Tokyo) 55:189-193. https://doi.org/10.2176/nmc.ra.2014-0307
3. Fujimura M, Tominaga T, Kuroda S et al (2022) 2021 Japanese Guidelines for the Management of Moyamoya Disease: Guidelines from the Research Committee on Moyamoya Disease and Japan Stroke Society. Neurol Med Chir (Tokyo) 62:165-170. https://doi.org/10.2176/jns-nmc.2021-0382
4. Kuroda S, Kashiwazaki D, Akioka N et al (2015) Specific Shrinkage of Carotid Forks in Moyamoya Disease: A Novel Key Finding for Diagnosis. Neurol Med Chir (Tokyo) 55:796-804. https://doi.org/10.2176/nmc.oa.2015-0044
5. Komiyama M, Ishiguro T, Nishikawa M, Yasui T, Morikawa T, Kitano S, Sakamoto H (2002) Constructive interference in steady state imaging of moyamoya disease. Neurol Med Chir (Tokyo) 42:11-16; discussion 17. https://doi.org/10.2176/nmc.42.11
6. Yamamoto S, Kashiwazaki D, Uchino H et al (2019) Stenosis Severity-Dependent Shrinkage of Posterior Cerebral Artery in Moyamoya Disease. World Neurosurg 126:e661-e670. https://doi.org/10.1016/j.wneu.2019.02.120

7. Yamamoto S, Kashiwazaki D, Akioka N, Kuwayama N, Noguchi K, Kuroda S (2019) Progressive Shrinkage of Involved Arteries in Parallel with Disease Progression in Moyamoya Disease. World Neurosurg 122:e253-e261. https://doi.org/10.1016/j.wneu.2018.10.001

8. Kuroda S, Fujimura M, Takahashi J et al (2022) Diagnostic Criteria for Moyamoya Disease - 2021 Revised Version. Neurol Med Chir (Tokyo) 62:307-312. https://doi.org/10.2176/jns-nmc.2022-0072

9. Uchino H, Ito M, Tokairin K, Tatezawa R, Sugiyama T, Kazumata K, Fujimura M (2023) Association of RNF213 polymorphism and cortical hyperintensity sign on fluid-attenuated inversion recovery images after revascularization surgery for moyamoya disease: possible involvement of intrinsic vascular vulnerability. Neurosurg Rev 46:119. https://doi.org/10.1007/s10143-023-02030-3

10. Hamano E, Kataoka H, Morita N, Maruyama D, Satow T, Iihara K, Takahashi JC (2017) Clinical implications of the cortical hyperintensity belt sign in fluid-attenuated inversion recovery images after bypass surgery for moyamoya disease. J Neurosurg 126:1-7. https://doi.org/10.3171/2015.10.JNS151022

11. Horie N, Morikawa M, Morofuji Y, Hiu T, Izumo T, Hayashi K, Nagata I (2014) De novo ivy sign indicates postoperative hyperperfusion in moyamoya disease. Stroke 45:1488-1491. https://doi.org/10.1161/STROKEAHA.114.004755

12. Takemoto Y, Kawano T, Ohmori Y et al (2020) Hemodynamic study about cortical hyperintensity belt sign after direct bypass surgery for moyamoya disease. J Clin Neurosci 74:124-129. https://doi.org/10.1016/j.jocn.2020.02.022

13. Uchino H, Yamamoto S, Kashiwazaki D, Akioka N, Kuwayama N, Noguchi K, Kuroda S (2019) Using postoperative remodeling of donor arteries on MR angiography to predict the development of surgical collaterals in moyamoya disease. J Neurosurg:1-9. https://doi.org/10.3171/2019.8.JNS191846

14. Uchino H, Kim JH, Fujima N et al (2017) Synergistic Interactions Between Direct and Indirect Bypasses in Combined Procedures: The Significance of Indirect Bypasses in Moyamoya Disease. Neurosurgery 80:201-209. https://doi.org/10.1227/NEU.0000000000001201

15. Fujimura M, Sonobe S, Nishijima Y, Niizuma K, Sakata H, Kure S, Tominaga T (2014) Genetics and Biomarkers of Moyamoya Disease: Significance of RNF213 as a Susceptibility Gene. J Stroke 16:65-72. https://doi.org/10.5853/jos.2014.16.2.65

16. Kawabori M, Ito M, Kazumata K et al (2023) Impact of RNF213 c.14576G>A Variant on the Development of Direct and Indirect Revascularization in Pediatric Moyamoya Disease. Cerebrovasc Dis 52:171-176. https://doi.org/10.1159/000526089

17. Ito M, Kawabori M, Sugiyama T et al (2022) Impact of RNF213 founder polymorphism (p.R4810K) on the postoperative development of indirect pial synangiosis after direct/indirect combined revascularization surgery for adult Moyamoya disease. Neurosurg Rev 45:2305-2313. https://doi.org/10.1007/s10143-022-01749-9

18. Uchino H IM, Sugiyama T, Kurisu K, Fujima N, Fujimura M (2025) Association between RNF213 p.R4810K and progression of cerebral artery negative remodeling in moyamoya disease. Neurol Med Chir (Tokyo)

19. Fujimura M, Tominaga T (2012) Lessons learned from moyamoya disease: outcome of direct/indirect revascularization surgery for 150 affected hemispheres. Neurol Med Chir (Tokyo) 52:327-332. https://doi.org/10.2176/nmc.52.327

20. Fujimura M, Kaneta T, Mugikura S, Shimizu H, Tominaga T (2007) Temporary neurologic deterioration due to cerebral hyperperfusion after superficial temporal artery-middle cerebral artery anastomosis in patients with adult-onset moyamoya disease. Surg Neurol 67:273-282. https://doi.org/10.1016/j.surneu.2006.07.017

21. Uchino H, Kuroda S, Hirata K, Shiga T, Houkin K, Tamaki N (2012) Predictors and clinical features of postoperative hyperperfusion after surgical revascularization for moyamoya disease: a serial single photon emission CT/positron emission tomography study. Stroke 43:2610-2616. https://doi.org/10.1161/STROKEAHA.112.654723

22. Kaku Y, Morioka M, Ohmori Y et al (2012) Outer-diameter narrowing of the internal carotid and middle cerebral arteries in moyamoya disease detected on 3D constructive interference in steady-state MR image: is arterial constrictive remodeling a major pathogenesis? Acta Neurochir (Wien) 154:2151-2157. https://doi.org/10.1007/s00701-012-1472-4

23. Ryoo S, Cha J, Kim SJ et al (2014) High-resolution magnetic resonance wall imaging findings of Moyamoya disease. Stroke 45:2457-2460. https://doi.org/10.1161/STROKEAHA.114.004761

24. Fukui M, Kono S, Sueishi K, Ikezaki K (2000) Moyamoya disease. Neuropathology 20 Suppl:S61-64. https://doi.org/10.1046/j.1440-1789.2000.00300.x

25. Kuroda S, Houkin K (2008) Moyamoya disease: current concepts and future perspectives. Lancet Neurol 7:1056-1066. https://doi.org/10.1016/S1474-4422(08)70240-0

26. Takagi Y, Kikuta K, Nozaki K, Hashimoto N (2007) Histological features of middle cerebral arteries from patients treated for Moyamoya disease. Neurol Med Chir (Tokyo) 47:1-4. https://doi.org/10.2176/nmc.47.1

27. Takagi Y, Hermanto Y, Takahashi JC et al (2016) Histopathological Characteristics of Distal Middle Cerebral Artery in Adult and Pediatric Patients with Moyamoya Disease. Neurol Med Chir (Tokyo) 56:345-349. https://doi.org/10.2176/nmc.oa.2016-0031

28. Kang HS, Kim JH, Phi JH et al (2010) Plasma matrix metalloproteinases, cytokines and angiogenic factors in moyamoya disease. J Neurol Neurosurg Psychiatry 81:673-678. https://doi.org/10.1136/jnnp.2009.191817

29. Fujimura M, Watanabe M, Narisawa A, Shimizu H, Tominaga T (2009) Increased expression of serum Matrix Metalloproteinase-9 in patients with moyamoya disease. Surg Neurol 72:476-480; discussion 480. https://doi.org/10.1016/j.surneu.2008.10.009

30. Narducci A, Yasuyuki K, Onken J, Blecharz K, Vajkoczy P (2019) In vivo demonstration of blood-brain barrier impairment in Moyamoya disease. Acta Neurochir (Wien) 161:371-378. https://doi.org/10.1007/s00701-019-03811-w

31. Hitomi T, Habu T, Kobayashi H et al (2013) Downregulation of Securin by the variant RNF213 R4810K (rs112735431, G>A) reduces angiogenic activity of induced pluripotent stem cell-derived vascular endothelial cells from moyamoya patients. Biochem Biophys Res Commun 438:13-19. https://doi.org/10.1016/j.bbrc.2013.07.004

32. Hamauchi S, Shichinohe H, Uchino H et al (2016) Cellular Functions and Gene and Protein Expression Profiles in Endothelial Cells Derived from Moyamoya Disease-Specific iPS Cells. PLoS One 11:e0163561. https://doi.org/10.1371/journal.pone.0163561

33. Fujimura M, Shimizu H, Inoue T, Mugikura S, Saito A, Tominaga T (2011) Significance of focal cerebral hyperperfusion as a cause of transient neurologic deterioration after extracranial-intracranial bypass for moyamoya disease: comparative study with non-moyamoya patients using N-isopropyl-p-[(123)I]iodoamphetamine single-photon emission computed tomography. Neurosurgery 68:957-964; discussion 964-955. https://doi.org/10.1227/NEU.0b013e318208f1da

34. Katsuki M, Fujimura M, Tashiro R, Tomata Y, Nishizawa T, Tominaga T (2021) Pre-operative higher hematocrit and lower total protein levels are independent risk factors for cerebral hyperperfusion syndrome after superficial temporal artery-middle cerebral artery anastomosis with pial synangiosis in adult moyamoya disease patients-case-control study. Neurosurg Rev 44:2191-2200. https://doi.org/10.1007/s10143-020-01395-z

35. Hayashi T, Yamamoto S, Hamashima T, Mori H, Sasahara M, Kuroda S (2021) Critical role of platelet-derived growth factor-alpha in angiogenesis after indirect bypass in a murine moyamoya disease model. J Neurosurg 134:1535-1543. https://doi.org/10.3171/2020.3.JNS193273

36. Nakamura M, Imai H, Konno K et al (2009) Experimental investigation of encephalomyosynangiosis using gyrencephalic brain of the miniature pig: histopathological evaluation of dynamic reconstruction of vessels for functional anastomosis. Laboratory investigation. J Neurosurg Pediatr 3:488-495. https://doi.org/10.3171/2008.6.PEDS0834

37. Yang Y, Torbey MT (2020) Angiogenesis and Blood-Brain Barrier Permeability in Vascular Remodeling after Stroke. Curr Neuropharmacol 18:1250-1265. https://doi.org/10.2174/1570159X18666200720173316

38. Kusaka N, Sugiu K, Tokunaga K et al (2005) Enhanced brain angiogenesis in chronic cerebral hypoperfusion after administration of plasmid human vascular endothelial growth factor in combination with indirect vasoreconstructive surgery. J Neurosurg 103:882-890. https://doi.org/10.3171/jns.2005.103.5.0882

39. Hiramatsu M, Hishikawa T, Tokunaga K et al (2017) Combined gene therapy with vascular endothelial growth factor plus apelin in a chronic cerebral hypoperfusion model in rats. J Neurosurg 127:679-686. https://doi.org/10.3171/2016.8.JNS16366

Statements and Declarations

Funding

This study was partially supported by Japanese Intractable Diseases Research Foundation grant number 2021B01 (HU), and Japanese Society for the Promotion of Science KAKENHI grant number 19H03765 (MI) and 20K09362 (MF).

Competing interests

The authors have no relevant financial or non-financial interests to disclose.

Author contributions

All authors contributed to the study conception and design. Material preparation, data collection and analysis were performed by Haruto Uchino and Masaki Ito. The first draft of the manuscript was written by Haruto Uchino. and all authors commented on previous versions of the manuscript. All authors read and approved the final manuscript.

Ethics approval

This study was approved by an Institutional Review Board at Hokkaido University Hospital (approval number 024-0257).

Consent to participate

Informed consent was obtained from all individual participants included in the study.

Consent to publish

Not applicable.

Table 1. Summary of clinical data

Characteristic	37 patients	42 hemispheres
Age, median (IQR), y	45 (39.5–65)	45 (38–52)
Male/female, n	27-Oct	10/32
Clinical presentation, n (%)		
Ischemia	34	38 (90%)
Hemorrhage	3	4 (10%)
RNF213 genotype, n (%)		
Homozygous, AA	0 (0%)	0 (0%)
Heterozygous, AG	23 (62%)	28 (67%)
Wild type, GG	14 (38%)	14 (33%)
Suzuki disease stage, median (IQR)	NA	3 (3–4)
Suzuki disease stage 1 and 2, n (%)	NA	8 (19%)
Suzuki disease stage 3 and 4, n (%)	NA	30 (71%)
Suzuki disease stage 5 and 6, n (%)	NA	4 (10%)
C1 outer diameter, median, mm	NA	2.39 (2.12–2.97)
FCH score, median (IQR)	NA	2.5 (1.75–4.0)
Direct bypass patent, n (%)	NA	42 (100%)
Favorable indirect bypass, n (%)	NA	27 (64%)

NA, not applicable; IQR, interquartile range; FCH, fluid-attenuated inversion recovery (FLAIR) cortical hyper intensity

Table 2. Correlation between clinical factors and indirect bypass development

Clinical factor	Indirect bypass development		Univariate analysis		Multivariate analysis	
	Favorable (n = 27)	Poor (n =15)	OR (95% CI)	P value	OR (95% CI)	P value
Median age, y	45	45	0.99 (0.94–1.05)	0.97		
Clinical presentation, n			0.41 (0.019–3.13)	0.44		
Ischemia	23	14				
Hemorrhage	4	1				
Disease stage, median	4	3	1.16 (0.62–2.28)	0.65		
RNF213 p.R4810K, n	17	10	1.06 (0.28–4.27)	0.93		
C1 diamter, median, mm	2.27	3.02	0.016 (0.00094–0.12)	0.0006	0.019 (0.0010–0.17)	0.0019
FCH score, median	3	2	1.72 (1.11–2.89)	0.022	1.15 (0.64–2.06)	0.62
Radiological hyperperfusion, n	7	2	2.27 (0.46–16.89)	0.34		

OR, odds ratio; CI, confidence interval; FCH, fluid-attenuated inversion recovery (FLAIR) cortical hyper intensity

Case 1

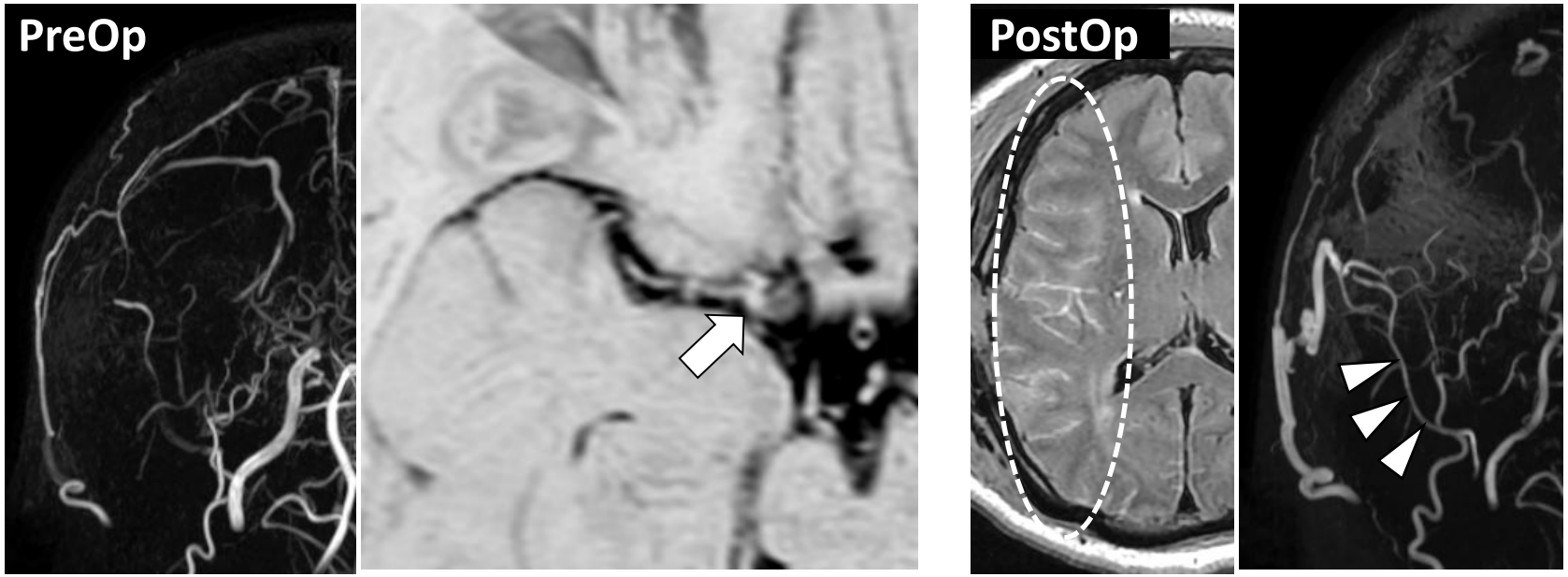

Case 2

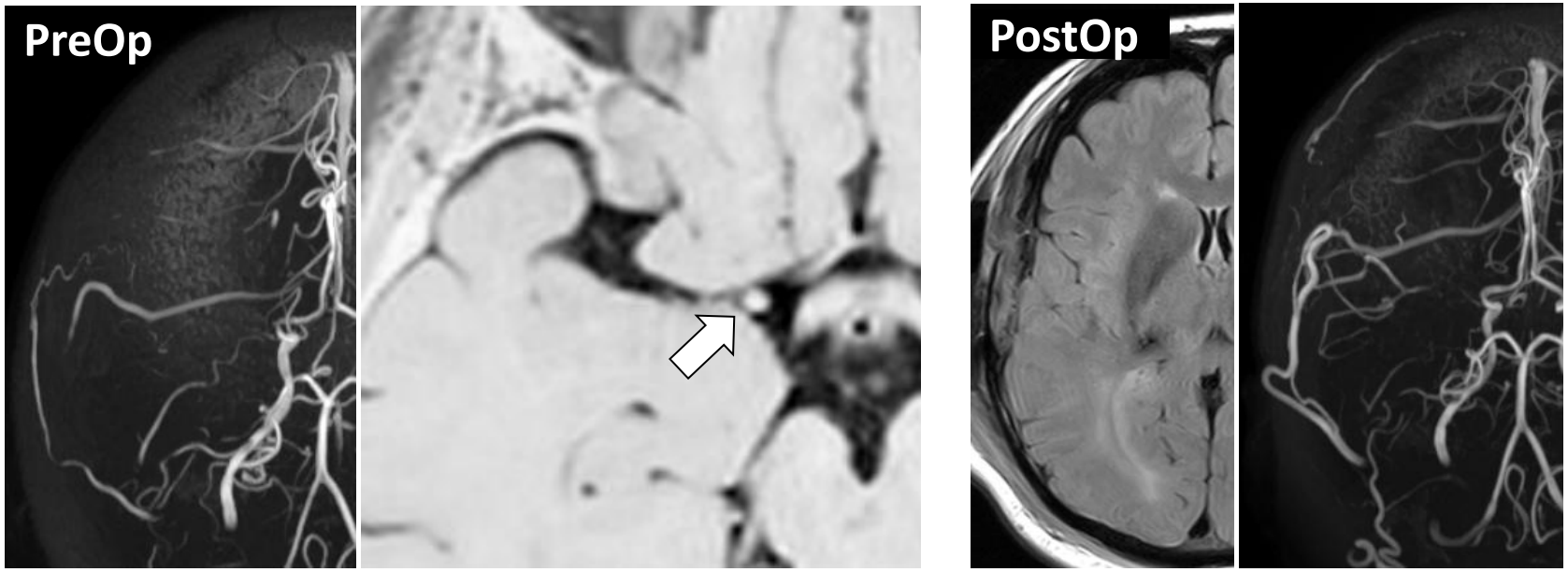

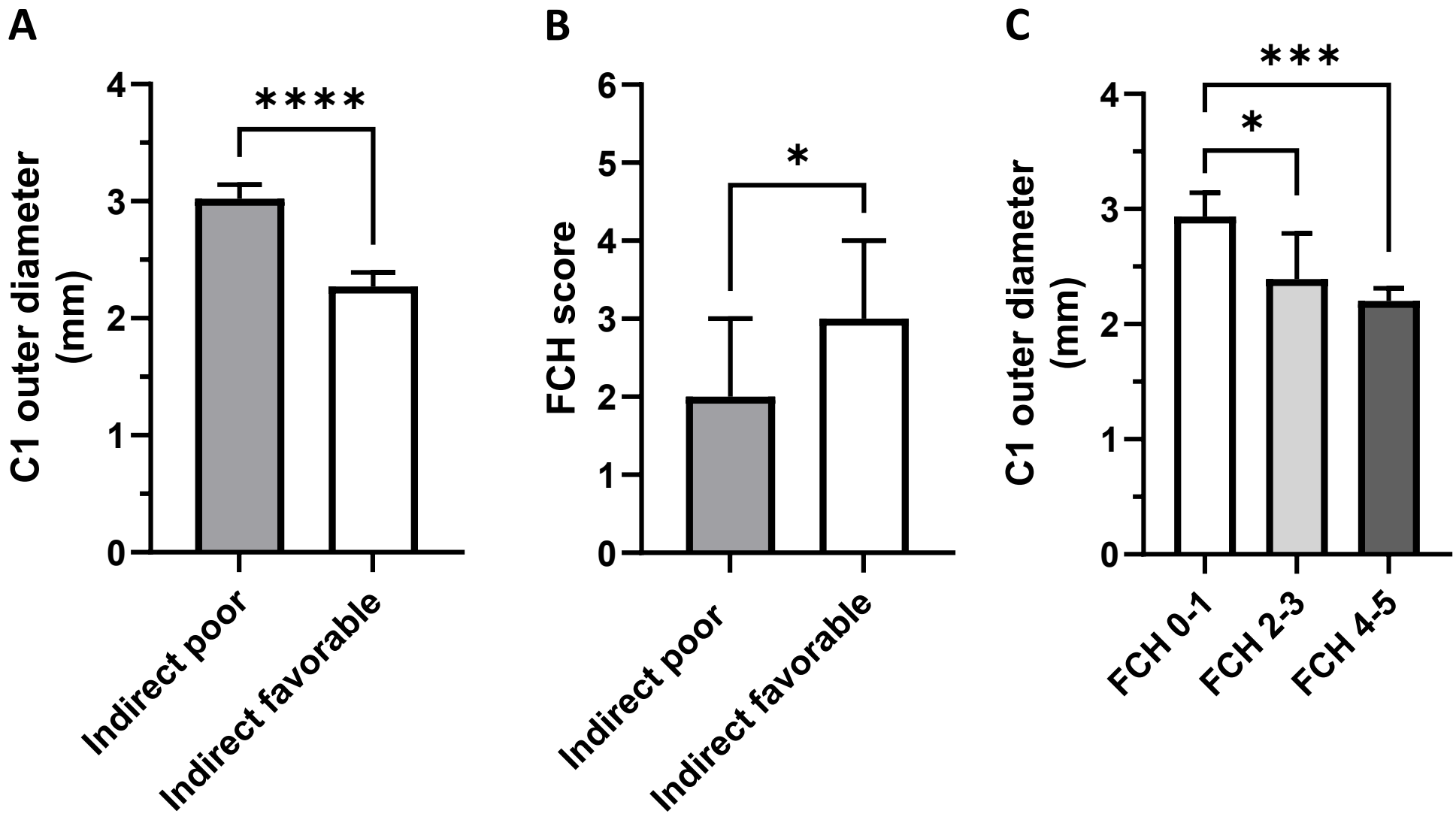
A
C1 outer diameter (mm)
****
Indirect poor
Indirect favorable
B
FCH score
*
Indirect poor
Indirect favorable
C
C1 outer diameter (mm)
***
*
FCH 0-1
FCH 2-3
FCH 4-5

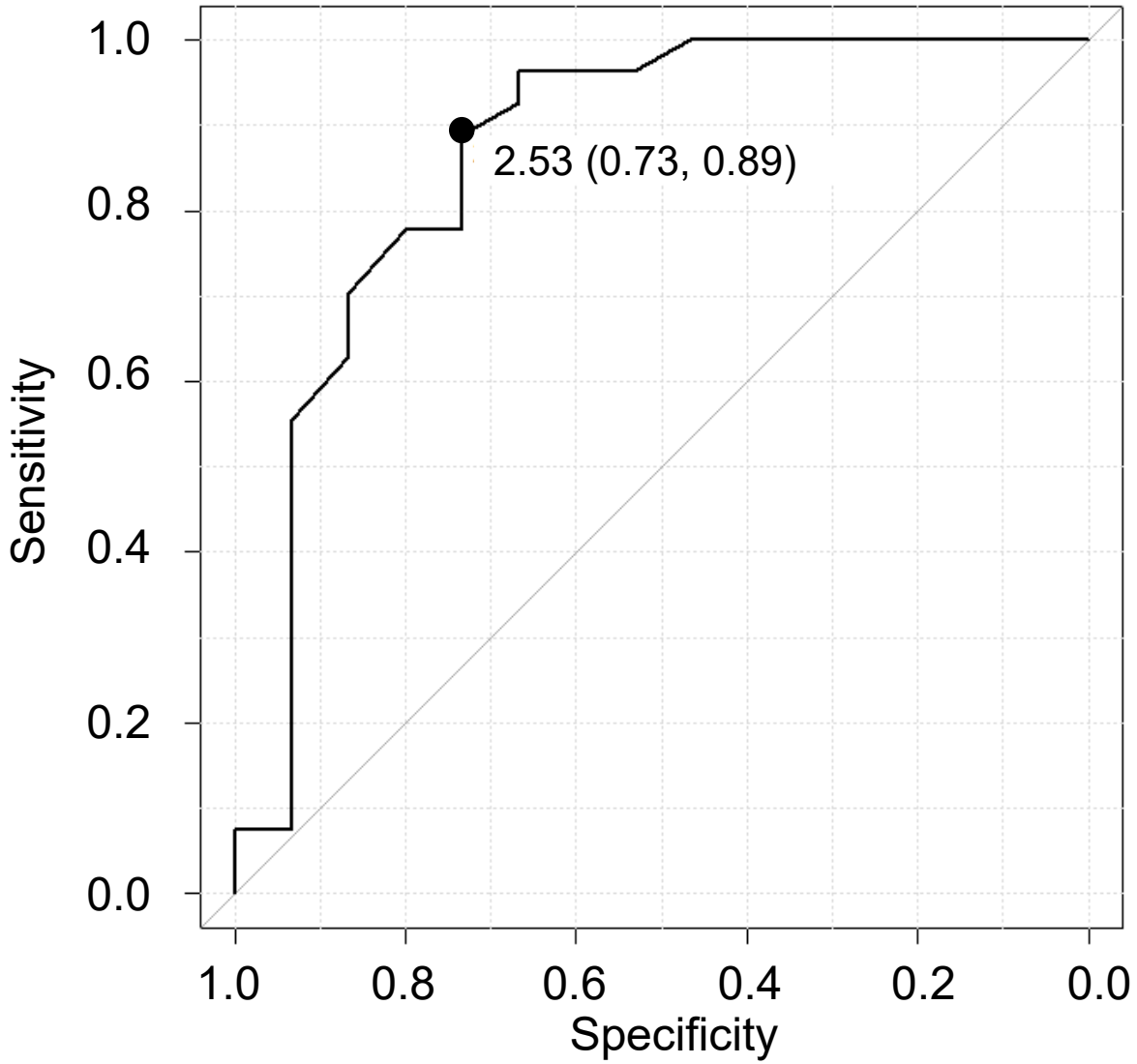
1.0
0.8
0.6
0.4
0.2
0.0
Sensitivity
2.53 (0.73, 0.89)
1.0
0.8
0.6
0.4
0.2
0.0
Specificity